Direct Measurement of Initial Wake Separation (b_o) and Initial Circulation (Γ_o) Using Pulsed Lidars

Hadi S. Wassaf
John A. Volpe National Transportation Systems Center, Cambridge MA, USA
hadi.wassaf@dot.gov

David C. Burnham
Scientific & Engineering Solutions Inc., Orleans MA, USA
dcburnham@scensi.com

Frank Y. Wang
John A. Volpe National Transportation Systems Center, Cambridge MA, USA
frank.wang@dot.gov

1. Introduction

The initial separation distance (b_o) between a counter-rotating vortex pair generated by an aircraft is a fundamental parameter affecting wake turbulence decay. For the past decade Pulsed Doppler Lidars have emerged as the primary remote sensors for measurement and characterization of wake vortices[1-5]. Unfortunately, b_o measurements are challenging using Pulsed Lidars in a traditional side-looking configuration. Such configuration introduces large errors due to poor range resolution but it is necessitated by the large standoff distance of pulsed Lidars[6]. In order to mitigate for this low range resolution the measured descent speed is usually used to infer the wake separation[7] b_o. This is however an inferred measurement that relies on a number of assumptions such as the weight and air speed of the aircraft. More recently, compact pulsed Lidars with short standoff distances for wind energy applications were introduced[8,9]. This paper describes a simple approach that makes use of this short standoff distance attribute by positioning the scanner directly under the aircraft's path in an upward looking Range Height Indicator (RHI) scan. Unlike the side-looking configuration, this scanning strategy leverages the high cross-range resolution and eliminates the range induced coupling between the aircraft vortex pair. This allows for a higher accuracy direct measurement of b_o and therefore minimizes the number of assumptions of unknown airplane parameters. When estimating the parameters of a vortex decay curve, a measurement of initial circulation Γ_o will further reduce the number of assumptions such as weight and air speed of the generating aircraft. The paper starts with the description of the measurement configuration and the algorithm used to extract b_o and initial circulation Γ_o A simulation of the vortices wind field and the Lidar signal is then used to validate the approach, as well as performing sensitivity analysis. Finally, an uncertainty analysis is performed to determine the minimum number of measurements needed to achieve a 2% accuracy for the b_o, Γ_o estimate.

2. Measurement Configuration and Algorithm Description

The scanner of a pulse Lidar is positioned on an extended runway centreline right under the approach path of a landing aircraft. The proposed nominal distance is about 4 nmi from touchdown so that the wakes generation height is approximately 1000'. This nominal distance is chosen so that the airplane path is already aligned with the runway, the aircraft is in landing configuration, and the generation height is large enough so that the wakes do not descend into the blind zone of the Lidar. An upward looking RHI scan configuration with the scan plane normal to the approach path is performed to extract the Line of Site (LOS) wind profile on a line joining the centroid of the two vortices. This geometry is depicted in the figure below.

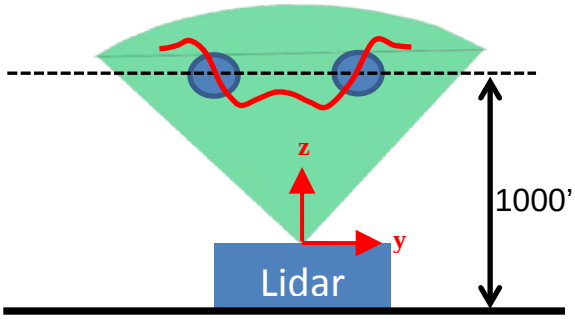

Figure 1: Lidar Measurement Configuration and wind profile extraction

The mean LOS wind velocity is found by taking the first moment of the signal spectrum corresponding to each range bin or Range

Gate (RG). The wake induced wind profile is extracted along a line joining the two wakes centroids (black dashed line of Figure 1). The velocity profile along this line is represented by the red trace in the same figure. This resulting LOS Mean velocity profile is used to estimate b_o and initial circulation after applying the appropriate corrections

3. Algorithm Description

At early age, the vortices have similar circulation strengths and altitudes. For a Burnham-Hallock[10] vortex model the velocity vector field can be expressed in the complex plane as follows

$$\boldsymbol{v}(\boldsymbol{r}) = j\frac{\Gamma_0}{2.\pi}.\left(\frac{\boldsymbol{r}-\boldsymbol{r_1}}{|\boldsymbol{r}-\boldsymbol{r_1}|^2+r_c^2} - \frac{\boldsymbol{r}-\boldsymbol{r_2}}{|\boldsymbol{r}-\boldsymbol{r_2}|^2+r_c^2}\right) \quad (1)$$

The Lidar senses the LOS component of the velocity field. This LOS velocity field is calculated as follows

$$v_{LOS}(\boldsymbol{r}) = j.\boldsymbol{v}^*(\boldsymbol{r}).\hat{\boldsymbol{r}}_{\boldsymbol{LOS}}(\boldsymbol{r})) \quad (2)$$

Where $\hat{\boldsymbol{r}}_{\boldsymbol{LOS}}(\boldsymbol{r})$ is the unit vector along the LOS direction to location $\boldsymbol{r}$, and $\boldsymbol{v}^*(\boldsymbol{r})$ denotes the complex conjugate of the velocity vector $\boldsymbol{v}(\boldsymbol{r})$. Consider a vortex pair with the following characteristics.

Γ_0	100 (m^2/s)
b_o	20 (m)
$\boldsymbol{r_1}$	-10+j.330 (m)
$\boldsymbol{r_2}$	+10+j.330 (m)
r_c	2.5 (m)

These quantities are used in equations (1) and (2) gives the LOS velocity field shown in the next figure below.

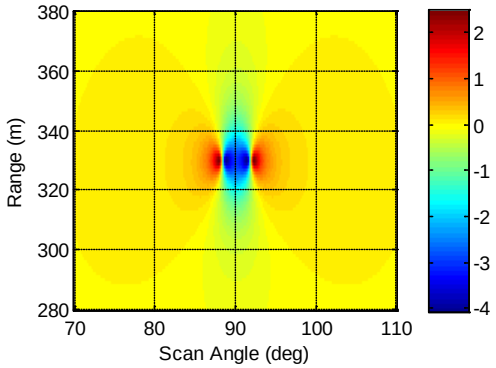

Figure 2: Wake induced LOS velocity profile at wakes altitude.

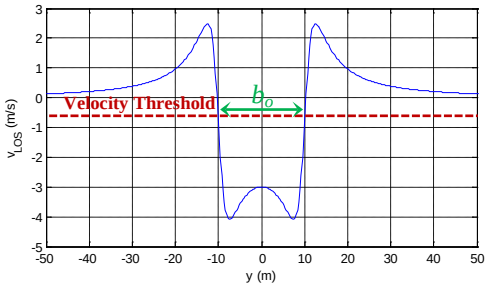

Figure 3: LOS induced velocity profile along a horizontal line at the wakes altitudes.

If the velocity profile $v_{LOS}(\boldsymbol{r})$ along a line joining the vortices centroids can be measured then using the velocity threshold in equation (3), b_o is lateral distance between the intersections of this threshold line and the measured profile as shown in equation (4) and illustrated in figure 3

$$v_{Th} = \frac{v_{LOS}(r_{v_{1,\max}}) - v_{LOS}(r_{v_{1,\min}})}{2} + \frac{v_{LOS}(r_{v_{1,\max}}) - v_{LOS}(r_{v_{1,\min}})}{2} \quad (3)$$

$$\boldsymbol{b_o} = \boldsymbol{r}(v_{LOS} = v_{Th})|_{real(r)<0} - \boldsymbol{r}(v_{LOS} = v_{Th})|_{real(r)<0} \quad (4a)$$

$$b_o = real(\boldsymbol{bo}) \quad (4b)$$

The circulation can also be calculated using this profile by inverting equations (1) and (2). In particular using the velocity at the center of the downwash region (y=0), the circulation becomes

$$\Gamma_0 = 2.\pi.v_{LOS}(\boldsymbol{r}).\left(\frac{b_o}{2} + \frac{r_c^2}{b_o}\right) \quad (5)$$

The downwash center location represents a good compromise between the desire to use a region of high velocity as well as low sensitivity to core size. In this geometry that uses a small b_o to look at worst case, varying the core size from 2 to 3 meters changes resulting Γ_o by less than 2.5%. Additional reasons for choosing the downwash is discussed later in this paper.
However, the Lidar measurements represent mean LOS velocities over the RG extent and not a high resolution velocity fields. This resolution degradation results in underestimated velocities and core enlargement. In order to assess these effects on the measured Γ_o and Γ_o, this velocity vector field is injected into a Distributed Target

Spectral LIdar Simulator (DT-SLIS) developed by Volpe, and the simulated Lidar measurements are compared to the high resolution input wind field to assess biases and compute any necessary corrections.

The emitted pulse is assumed to have the following Gaussian envelope.

$$A_L(t) = \frac{1}{(2\pi\sigma^2)^{\frac{1}{4}}} e^{-\frac{\frac{1}{4}t^2}{\sigma^2}} \quad (6)$$

The spectral model[2,11-13] used in this simulator is

$$\hat{S}_{nz}(f) = B.SNR(z_o) \int_{-\infty}^{\infty} Q'(z).\, e^{-\frac{1}{2}\frac{\left(f+\frac{2}{\lambda}V_r(z)\right)^2}{\sigma_{fb}^2}} dz + 1 \quad (7a)$$

With $\sigma_{fb} = \sqrt{\sigma_f^2 + \left(\frac{1}{3T}\right)^2}$ (7b)

And $\sigma_f = \frac{1}{4\pi\sigma}$ (7c)

The function *Q'(z)* Defines the radial extent of the sensing volume or RG and has the following form:

$$Q'(z) = 2\sqrt{2\pi}\,\sigma.Q(z) \quad (8a)$$

$$Q(z) = \frac{1}{cT}\left\{\mathrm{erf}\left(2\frac{z_0-z}{\sqrt{2}c\sigma} + \frac{T}{2\sqrt{2}\sigma}\right) - \mathrm{erf}\left(2\frac{z_0-z}{\sqrt{2}c\sigma} - \frac{T}{2\sqrt{2}\sigma}\right)\right\} \quad (8b)$$

And it shows that the RG resolution is defined by both pulse width σ and the *FFT* window duration T.
The simulation parameters are tabulated below

N_{FFT}	*128*
$N_{FFT\_NoZeroPadding}$	*7*
SSB_Flag	*1*
λ	*1.565 (μm)*
f_s	*83.33 (Mhz)*
B	*83.33 (Mhz)*
σ	*39 (ns)*
$\mu_{PSD(Noise)}$	*1 (Unit/Hz)*
$\sigma_{PSD(Noise)}$	*.2 (Unit/Hz)*
PSD_{Thresh}	$5.\sigma_{PSD(Noise)}$
SNR	*7 (Linear)*

N_{FFT} is the size of the FFT window including data samples and zero padding, $N_{FFT\_NoZeroPadding}$ is the number of actual data samples in the FFT window, *SSB_Flag* indicates whether the time series is real or a complex single sideband signal. λ is the optical wavelength, f_s is the sampling frequency of the A/D, *B* is the analog filter bandwidth, σ is the width of the Gaussian pulse defined in equation (6), $\mu_{PSD(Noise)}$ is the PSD noise floor , $\sigma_{PSD(Noise)}$, is characterizes the white fluctuations on the PSD noise floor. These fluctuations lose whiteness as the spectrum is convolved with the fourier transform of the FFT window. PSD_{Thresh} is the threshold applied prior to calculating the spectrum first moment (or mean LOS wind), SNR is the linear narrowband SNR and is based on an assumed Backscatter and extinction coefficients.
The measured LOS velocity field output of the simulator is shown below.

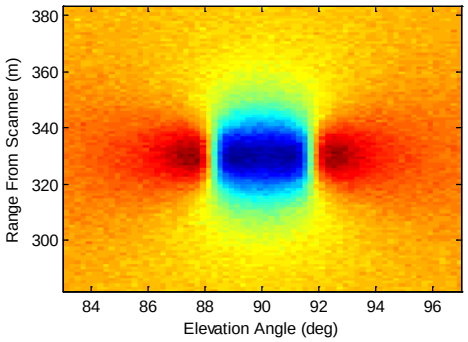

Figure 4: Measured LOS velocity field as outputted by DT-SLIS.

As the beam scans across both vortices the maximum wind speeds are approximately at equal ranges from the scanner. If the wake pair centre has a lateral offset relative to the Lidar scanner and/or the vortex pair is slightly tilted then the range from the scanner to the maximum LOS velocity point will vary with angle. Therefore, the line along which the profile is extracted is found by performing a robust linear fit through the ranges $R_{MAx}(\theta)$ to the maximum wind velocities as function of LOS elevation angle θ. The resulting measured velocity profile output from D-SLIS at the wake altitudes is super-imposed on the input LOS velocity profile in the figure below.

`

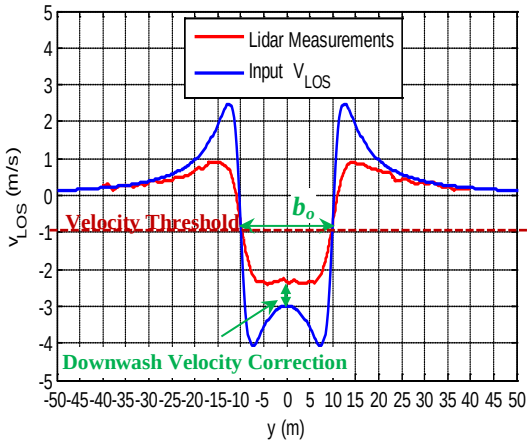

Figure 5: Overlaid input and measured LOS Velocity profiles along a horizontal line at wakes altitude.

This Figure shows that, as expected, the Lidar underestimates the wake induced velocity field. The measured velocity approaches the true LOS velocity as the measurement volume moves further from either vortices cores and become practically the same as 30 meters away from either cores. However, at these distances velocities are small and cannot be accurately measured as they become buried in the ambient atmospheric turbulence field which are not part of this simulation. We will now investigate the implication of these LOS velocities underestimates on the two quantities of interest: the initial circulation Γ_0 and the wake separation b_0. In order to estimate Γ_0, the region that has the smallest bias and largest LOS velocity should be used in order to minimize the effects of atmospheric turbulence on the resulting estimate. This region is clearly the centre of the downwash. Figure 5 also shows that the peaks are completely smeared out in the DT-SLIS measurement output so that it is a flat plateau and therefore the result is not significantly impacted if the circulation is estimated from a velocity that is not exactly at the centre of the downwash region. The algorithm exploits this fact by taking an average velocity of the measured downwash region to significantly reduce measurement noise and apply a correction equal to the difference between the centre of the downwash velocity of the blue trace and the red trace. For this particular geometry, the simulation shows that a correction factor of 1.3 should be used.

The second quantity of interest is b_o. Despite the smearing of the downwash peaks and the underestimate of velocities, this simulation shows that the centroids of both wakes are still accurately estimated as the midpoint between the measured downwash and peak velocities. However, the underestimated velocities along with core enlargement in the measured profile increase the sensitivity of b_0 to errors in the choice of the threshold this affects the minimum data sample size required to accurately estimate b_o. This is quantified later in the measurement uncertainty section of this paper.

3. Sensitivity to Scan Elevation Angle

The simulation results presented so far show that when the vortex pair centroid is right above the scanner (at a lateral coordinate y=0) the b_0 measurement is unbiased, and a correction on the order of 1.3 should be applied to the $\Gamma_o$measurements. However, this case is relevant only under near zero wind conditions. In reality these wakes are measured under non-zero wind conditions for approximately 30 to 40 seconds after the airplane crosses the scan plane. In order to control the maximum lateral transport within the measurement time window, the maximum acceptable wind is restricted to below 3 m/s. this results in a maximum scanner elevation angle to the vortex pair centroid of approximately 20° from vertical (70° to 120°). DT-SLIS is run for vortex pair centroid scan angles between 90° and 150° with 2° increment between consecutive runs. And the wind field from each simulation run is used to compute the Γ_o correction angles. The results are shown in Figure 6. Since the correction factor is symmetrical about 90° only angles>90° are plotted.

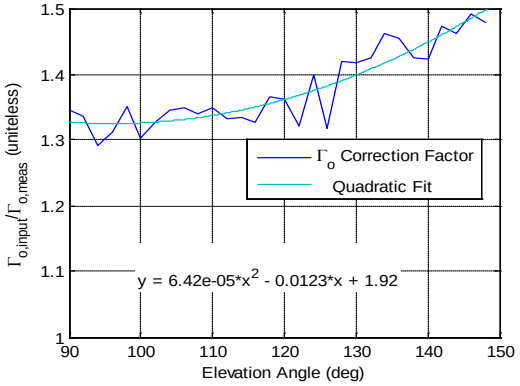

Figure 6: Correction factor for the measured circulation as a function of scan angle to the vortex pair centroid. Standard deviation of the residual error after correction is <2.5%.

The quadratic fit to the corrections varies from 1.33 to 1.36 with a residual error standard deviation <2.5%. If we restrict our attention to the angles of interest (90° to 120°), this error is <2%

The b_o correction factor is also estimated from the same simulation runs. The results are shown below

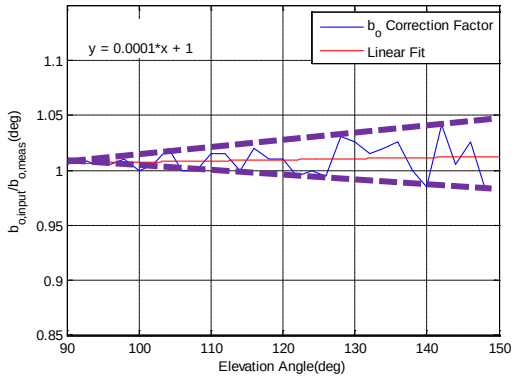

Figure 7: Correction factor for the measured b_o as a function of scan angle to the vortex pair centroid. Effectively no correction is required and the standard deviation of the error is 1.6%.

Figure 7 shows no significant bias (and therefore no correction is needed) for b_o measurements. However the uncertainty on the measurement grows as the angel from the vertical gets larger. The error standard deviation is 1.6% for (90^o to 150^o). For the angles of interest (90^o to 120^o) this error drops to 1%.

4. G_o and b_o Measurement Uncertainty

The simulation results above indicate that the proposed algorithm, when applied to the Lidar measurements can produce accurate b_o and Γ_o(after applying the appropriate correction). However, this assumes perfect crosswind correction, no background atmospheric turbulence, and no up or down drafts. These effects will introduce measurement uncertainties and are here discussed individually

a. Atmospheric Turbulence Effects

The small scale atmospheric turbulence tends to increase the noise on the flow field. Since the circulation is estimated by taking the average of the downwash region, the turbulence effect is mitigated by the averaging process. In the case of b_o this effect can be modelled as error in the threshold estimate.

Assume the error in threshold to be Gaussian distributed with a mean equal to the correct threshold and with a standard deviation σ_E equals to one-sixth the difference between the peak and downwash velocities. This ensures that the threshold is below the peak value and above the downwash velocity value with a probability grater than 0.995. Since the difference between these two velocities in this simulation is $3.3\ m/s$, then $\sigma_E = 0.55\ m/s$.

Since the velocity transitions between a peak and the downwash are near linear, the resulting b_o distribution will also be Gaussian. Instead of approaching the problem analytically, the threshold is randomized in a Monte Carlo mode for $N = 10^5$ iterations, and the resulting distribution of b_o values is shown below

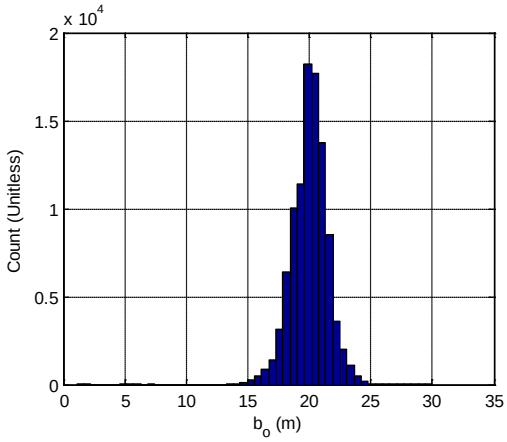

Figure 8: Histogram of bo estimates from the same measured profile by randomizing the velocity threshold.

As expected, this distribution is approximately Gaussian, with a standard deviation $\sigma_{bo} = 1.4\ m$ or 7% of b_o. For a scan duration of 15 seconds or less, b_o can be assumed constant in the first two consecutive scans after roll up, and these two measurements are therefore averaged to get the final b_o estimate. If the threshold error is assumed independent from scan to scan then this results in an effective b_o uncertainty of

$$\frac{\sigma_{bo}}{b_o} = \frac{.07}{\sqrt{2}} = 5\% \qquad (9)$$

b. Crosswind Correction Error

In the case of real measurements, the crosswind is estimated by calculating the wakes' velocities from two consecutive scans. Vertical wind is assumed zero or estimated from Lidar measurements using a vertical beam prior to an aircraft passage. The residual error in crosswind measurements E_{uy} introduces an error in b_o equals E_{bo}.

$$E_{bo} = E_{uy}.\Delta t \qquad (10)$$

If E_{uy} is assumed to be zero mean Gaussian distributed with a standard deviation σ_{uy} then the crosswind error induced uncertainty on b_o is given by

$$\sigma_{bo} = \sigma_{uy}.\Delta t \quad (11)$$

The time Δt is the time taken to scan across the peaks from both vortices.

Equation (11) indicates that the larger the scan time between the two vortices, the larger is the effect of wind error on the measured b_o.

Since vortices move with the wind throughout the scan, this time Δt is a function of crosswind u_y and is approximately given by

$$\Delta t = \frac{b_o}{|V_{Sy} - U_y|} \quad (12)$$

Where V_{Sy} represents the lateral velocity of the beam at the vortex altitude and can be considered approximately constant for small angles from the vertical

$$V_{Sy} = R.\dot{\theta_s} \text{ (for } \theta_s \text{near } 90^o) \quad (13)$$

Equation (12) shows that Δt is largest when the scanner and wind velocities are in the same direction and smallest when these two velocities are in opposite directions as expected. If the maximum crosswind measurement conditions are restricted to $U_y < 3\ m/s$ then for a scanner speed $\dot{\theta_s} = 2$ (^{o}/sec) and an altitude of 300 m (~1000'), the beam velocity at wakes altitude is $V_{Sy} = 10.5\ m/s$, and the travel time between peaks are

$$\Delta t_{max} = \frac{20}{7.5} = 2.67\ sec \quad (14a)$$

For beam and crosswind velocities in the same direction (Forward-stroke), and

$$\Delta t_{min} = \frac{20}{13.5} = 1.5\ sec \quad (14b)$$

for beam and crosswind velocities in opposite directions (Back-stroke).

Assuming the wind can be measured with a 20% uncertainty, then $\sigma_{uy} = .6\ m/s$. Using this value along with equations (14a,b) in equation (11) we get the wind induced uncertainty bounds.

$.9m < \sigma_{bo} <$ 1.6m

If the b_o value is averaged from two consecutive scans then the uncertainty becomes

$$\sigma_{bo} = \sqrt{\frac{.9^2+1.6^2}{2}} = 1.3 \text{ m} \quad (15)$$

The relative uncertainty for an average of 2 scans is therefore

$$\frac{\sigma_{bo}}{b_o} = 6.5\% \quad (16)$$

For small elevation angles from the vertical, crosswind error has no significant contribution to the downwash and circulation measurements are therefore not affected.

c. Vertical Wind Correction Error

The vertical wind velocity effects on b_o estimate can be neglected since it biases the velocity peaks and downwash in the same direction. The threshold which is the average between the peaks and the downwash will therefore still capture the vortices centroids.

The circulation however is determined only by the downwash as described in equation (5). For a vertical wind standard deviation of 0.3 m/s (chosen to be half of the crosswind error), the uncertainty on Γ_0 is found as follows

$$\frac{\sigma_{\Gamma o}}{\Gamma_o} = \frac{2.\pi.\sigma_{vo}.\left(\frac{b_o}{2}+\frac{r_c^2}{b_o}\right)}{100} = 19\% \quad (17)$$

d. Minimum Sample Size

Assuming the measurement errors described above are independent, then the total measurement uncertainty for b_o can be found by combining the 1% residual error from the angular sensitivity analysis with equations (9) and (16) as follows

$$\frac{\sigma_{bo,Total}}{b_o} = \sqrt{.01^2 + .05^2 + .065^2} = 8.3\% \quad (18)$$

If an uncertainty of 2% is required then the number of independent measurements for the same aircraft type and configuration is

$$N_{meas,bo} = \left(\frac{0.083}{.02}\right)^2 = 18$$

The number of independent measurements required to meet an accuracy of 2% on Γ_o is found by combining the 1.25% error from core size effects, 2% residual error (after applying the correction factor), and equation (17) as follows

$$N_{meas,Go} = \left(\frac{\sqrt{.125^2 + .2^2 + 0.19^2}}{.05}\right)^2 = 92$$

Therefore, an approximate number of 92 good measurements are needed to meet the

accuracy requirement for both Γ_o and b_o. With this number of measurements the required accuracy of b_o alone is significantly exceeded.

5. Conclusion

A new direct approach to measuring the separation between 2 airplane wake vortices using the mean wind measurements from a short pulse Lidar in an upward looking RHI configuration was presented. The simulation analysis showed that initial circulation $\Gamma_o$can also be accurately measured after applying a correction factor. The correction factor was calculated as a function look angle to the Vortex pair centre and varies from 1.33 to 1.36 for the angles of interests. The simulation shows that there are no significant biases in the b_o measurement. The uncertainty analysis performed shows that 92 measurements per airplane type and configuration are approximately needed to meet the required uncertainty bounds of 2% for both circulation and b_o measurement uncertainties. The future work will focus on the analysis of real measurement data and use it to build airplane specific circulation decay curves

6. Acknowledgements

The authors would like to Jeff Tittsworth of the FAA Wake Turbulence Program for his continued support of this work.

7. References

1. D. Jacob et al. “Development of an Improved Pulsed Lidar Circulation Estimation Algorithm and Performance Results for Denver OGE Data”, 52st AIAA Aerospace science meeting, Dallas, Texas, Jan 2013: AIAA 2013-0509.
2. H. S. Wassaf et al. “Wake Vortex Tangential Velocity Adaptive Spectral (TVAS) Algorithm for Pulsed Lidar Systems”, 16th CLRC meeting, Long Beach, California, (2011).
3. J. A. Thomson,. and S. M. Hannon. "Wake Vortex Modeling for Airborne and Ground Based Measurements Using A Coherent Lidar", Society of Photo-Optical Instrumentation Engineers (SPIE) Proceedings 2464, Orlando, FL, 1995: 63-78
4. F. Köpp et al., “Characterization of Aircraft Wake Vortices by 2-mm Pulsed Doppler Lidar”, Journal of Atmospheric and Oceanic Technology 21, (2004): 194:206
5. S. Rahm and I. Smalikho. “Aircraft Wake Measurement with Airborne Coherent Doppler Lidar”, Journal of Aircraft 45.4 (2008): 1148-1155.
6. S. Hannon, “Pulsed Doppler Lidar For Terminal Area Monitroing Of Wind Aand Wake Hazards”, 11th Conference on Aviation, Range, and Aerospace Meteorology, Hyannis, MA October (2004),
7. Delisi, D. P. et al. “Estimates of the Initial Vortex Separation Distance, bo, of Commercial Aircraft from Pulsed Lidar Data”, AIAA Aerospace Sciences Meeting, Dallas, Texas (2013): AIAA2013-0365
8. Cariou j. p. et al. “Long range scanning pulsed Coherent Lidar for real time wind monitoring in the Planetary Boundary Layer”, 16th CLRC meeting, Long Beach, California, (2011)
9. T. Ando et al. “All-fiber Coherent Doppler LIDAR technologies at Mitsubishi Electric Corporation”, 14th International Symposium for the Advancement of Boundary Layer Remote Sensing, (2008): 012011
10. D. C. Burnham and J. N. Hallock “Decay Characteristics of Wake Vortices from Jet Transport Aircraft”, Journal of Aircraft. 50, No. 1 (2012): 82-87
11. P. Salamitou et al., “Simulation in the time domain for heterodyne coherent laser radar”, Applied Optics, 34.3, (1999): 499-506,.
12. R. G. Frehlich and M. J. Kavaya, “Coherent Laser Radar Performance For General Atmospheric Refractive Turbulence”, Applied Optics, 30, No. 36, 5325-5352, (1991).
13. V. A. Banakh and I. N. Smalikho, “Estimation of The Turbulence Energy Dissipation Rate From The Pulsed Doppler Lidar Data”, Atmos. Oceanic Optics 10, No. 12, 957-965, (1997).